Neuron, Vol. 17, 1221–1229, December, 1996, Copyright ©1996 by Cell Press

Determinants of Nicotinic Receptor Gating in Natural and Unnatural Side Chain Structures at the M2 9′ Position

Patrick C. Kearney,* Haiyun Zhang,† Wenge Zhong,‡ Dennis A. Dougherty,‡ and Henry A. Lester*
*Division of Biology
†Division of Physics, Mathematics, and Astronomy
‡Division of Chemistry and Chemical Engineering
California Institute of Technology
Pasadena, California 91125

Summary

A nonsense suppression method was employed to incorporate a total of four natural and six unnatural residues at the 9′ position of the M2 region in the β, γ, and δ subunits of muscle nicotinic receptors. In 33 pairwise comparisons of functional properties as influenced by structural features including side chain length, branching, and substitution of oxygen for methylene carbons, it is concluded that increased polarity in the side chains at the 9′ position consistently increases the sensitivity to acetylcholine. In addition, the stereochemistry of the side chain can have marked influences on the EC_{50}, primarily because of changes in the single-channel open time. For the case of isoleucine versus *allo*-isoleucine in the δ subunit, these changes are themselves modified by mutations at the 9′ position in other subunits. The data suggest an especially strong interaction between the β and δ subunits in the pore region, leading in turn to a suggested arrangement of subunits within the pentamer.

Introduction

Modern electrophysiological techniques bring detailed resolution to the study of ion channel gating. An important goal is to relate these functional measurements to the structure of the side chains thought to move during channel opening and closing. It is particularly appropriate to study the role of a highly conserved leucine in the M2 domain of nearly all known subunits of nicotinic acetylcholine receptors (nAChRs). In one numbering system, the leucine residues align at the 9′ position in the M2 region (Figure 1; see also Charnet et al., 1990). There is evidence that these residues, as well as nearby residues at 6′ and 10′, contribute to the conducting pathway (Giraudat et al., 1986; Leonard et al., 1988; Charnet et al., 1990; Akabas et al., 1992). In one interpretation of structural data at 9 Å resolution, the five 9′ side chains (one each from the two α, the β, the γ, and the δ subunits) form an axial constriction that prevents current flow through the closed channel. Channel opening is accompanied by movement of these 9′ leucine residues, removing the physical block to conduction (Unwin, 1995). Other structural models also posit a crucial role in gating for the 9′ residues (Karlin and Akabas, 1995).

Despite the high conservation of the 9′ leucine, many other residues produce functional receptors at this position (Revah et al., 1991; Bertrand et al., 1992), allowing site-directed mutagenesis experiments that gather detailed comparative information. Mutations at this position show that, to first approximation, each leucine governs gating in an independent and symmetrical manner (Filatov and White, 1995; Labarca et al., 1995). However, detailed analysis of the earlier mutagenesis data suggests that individual mutations are not identical, as though some subunit pairs have a special relationship.

We reasoned that this interesting position, and these possible interactions, could profitably be studied with the in vivo nonsense codon suppression technique of unnatural amino acid mutagenesis, which allows the introduction of a practically unlimited range of side chain structures. We report here that many side chains, including those derived from both natural and unnatural amino acids, produce functional receptors when expressed at the 9′ position. Expression is sufficiently high to enable single-channel studies with the nonsense suppression technique; previously, single-channel measurements on gating with unnatural residues were possible only with completely synthetic channels such as gramicidin (Oiki et al., 1995). In a particularly complete series of results, EC_{50} is increased by several different substitutions that increase hydrophobicity, emphasizing the importance of polar interactions at the 9′ position. Furthermore, even subtle changes such as the stereochemistry of the side chain can produce marked changes in gating as evaluated by either steady-state or kinetic measurements; and these changes are themselves influenced by other subunits in a way that suggests direct physical interactions and an ordering of the subunits.

Results

Figure 2 presents structures and EC_{50} values (ACh) for the four natural and six unnatural side chains that we have incorporated at the 9′ position in the M2 domain of the mouse muscle nAChR β, γ, and δ subunits. For all the side chains tested, receptors displayed robust responses (whole oocyte currents >500 nA for high [ACh]). There were no major differences between the two groups, natural versus unnatural, with regard to response amplitude, range of EC_{50} values (1.2–77 μM versus 5.3–79 μM), mean EC_{50} (30.5 μM versus 31.8 μM), range of Hill coefficients (1.66 to 1.81 versus 1.66 to 1.88), or mean Hill coefficient (1.73 for both groups). These EC_{50} values encompass a favorable range for quantitative measurements; there is little interference from channel block that occurs at high [ACh] in studies of AChR mutants with EC_{50} values > 200 μM, or from spontaneous openings that occur at AChR mutants with EC_{50} values < 1 μM (Labarca et al., 1995). Furthermore, the Hill coefficients approaching 2 show that for these receptors, as for wild-type AChRs, the open state of the channel is much more likely to be associated with the presence of two bound agonist molecules than with a single bound agonist molecule. We show in a later section that several receptors in this series also have nearly

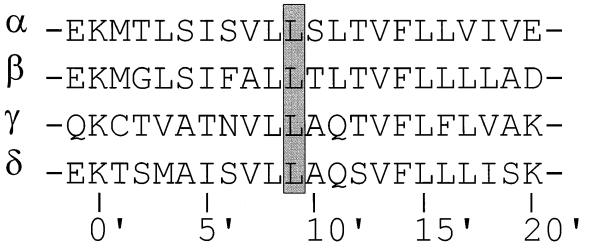

Figure 1. Sequences of the M2 Region for the Four Subunits of the Mouse Muscle nAChR

The putative N-terminus of the M2 region is assigned the position 1′ (Charnet et al., 1990). This study emphasizes the highly conserved leucine residue at 9′.

normal single-channel conductances and open times. Thus, AChRs with these unnatural amino acids at the M2 9′ position display several nearly normal functional characteristics.

Side Chain Polarity at 9′ Partially Controls Agonist Sensitivity

Figure 3A presents a classification of incremental changes in side chain properties. The data provide a number of ways to test for consistency with the notion that hydrophobicity of the 9′ residues influences gating. We can increase hydrophobicity by adding a single CH_2 group, either by increasing chain length (row 1), by β-branch addition (row 2), or by γ-branch addition (row 3). Alternatively, we can increase hydrophobicity without significantly affecting the sterics of the side chain, by converting a polar oxygen to a nonpolar CH_2 group (row 4). In all, these series involve 11 pairwise comparisons among the 10 residues studied; because each residue was tested at position 9′ in the β, γ, and δ subunits, there are 33 pairwise comparisons. As tabulated in Figure 3B, the overall data set produces a consistent picture that increasing hydrophobicity raises EC_{50}. The data are quantified by the statement that the grand averages, in the final column of the table, all exceed unity. For each class of structural change, the data are consistent in the sense that all but one of six or nine individual component ratios also exceed unity. The -O- to -CH_2- change (row 4) produces the largest effect, on average a factor of almost 6 in EC_{50} (a nearly equal value, 5.7, is obtained if the average is performed logarithmically rather than linearly). It is striking that the isosteric changes of row 4 produce changes almost comparable (6-fold versus 10-fold) to the much more disruptive 9′ leucine to serine mutation, suggesting that polarity is the major determinant.

Addition of a CH_2 (rows 1, 2, and 3 in Figure 3A) produces a smaller effect, but clearly in the direction that increased hydrophobicity leads to a higher EC_{50}. Within the three series that represent this class of structural change, the effect of γ branching is smallest (row 3); the grand average is 1.3, and no individual ratio exceeds 2. The effect of increasing chain length is largest; the grand average is 1.8, and several individual ratios exceed 2. To compare the subunits with respect to the effect of a CH_2 addition, we have calculated the vertical averages of the EC_{50} ratios in rows 1–3. These averages range between 1.4 and 1.7, showing that the β, γ, and δ subunits respond roughly equally to the structural changes that increase hydrophobicity.

Side Chain Stereochemistry Also Affects EC_{50} and Channel Duration

We have tested further to discern other effects of side chain structure. A clear pattern emerges when side chain

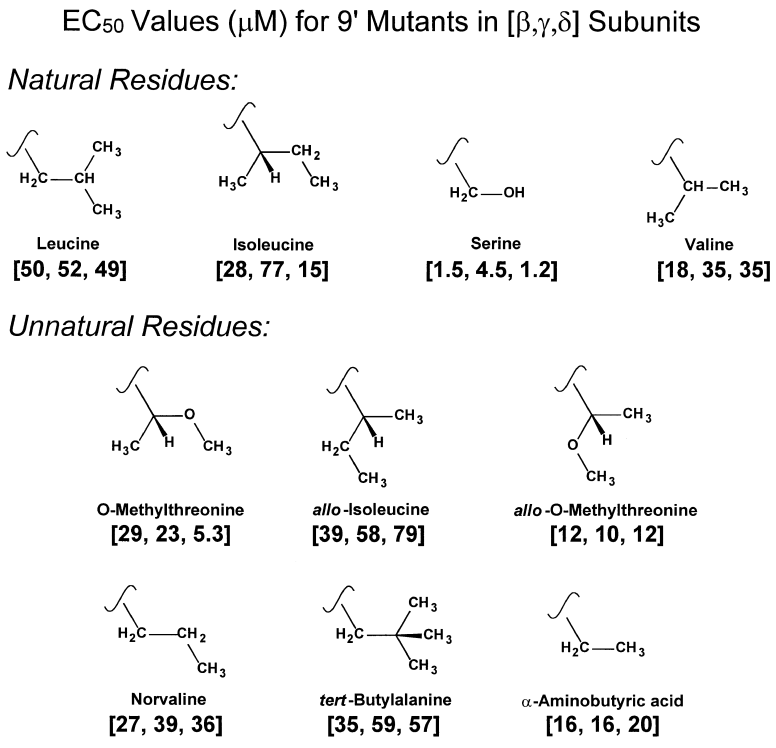

Figure 2. Structures and EC_{50} Values for Receptors Tested by Nonsense Suppression at a Single 9′ Residue with Four Natural and Six Unnatural Residues

Natural (top row); unnatural (bottom two rows). The wild-type (WT) is leucine at each subunit (see Figure 1). Each mutant differs from the WT by a single residue in a single subunit. Values in brackets are the EC_{50} values (μM) for incorporation at the β, γ, or δ subunits respectively. The values have an SEM of ±5%. EC_{50} values for double mutants are given in later figures.

A

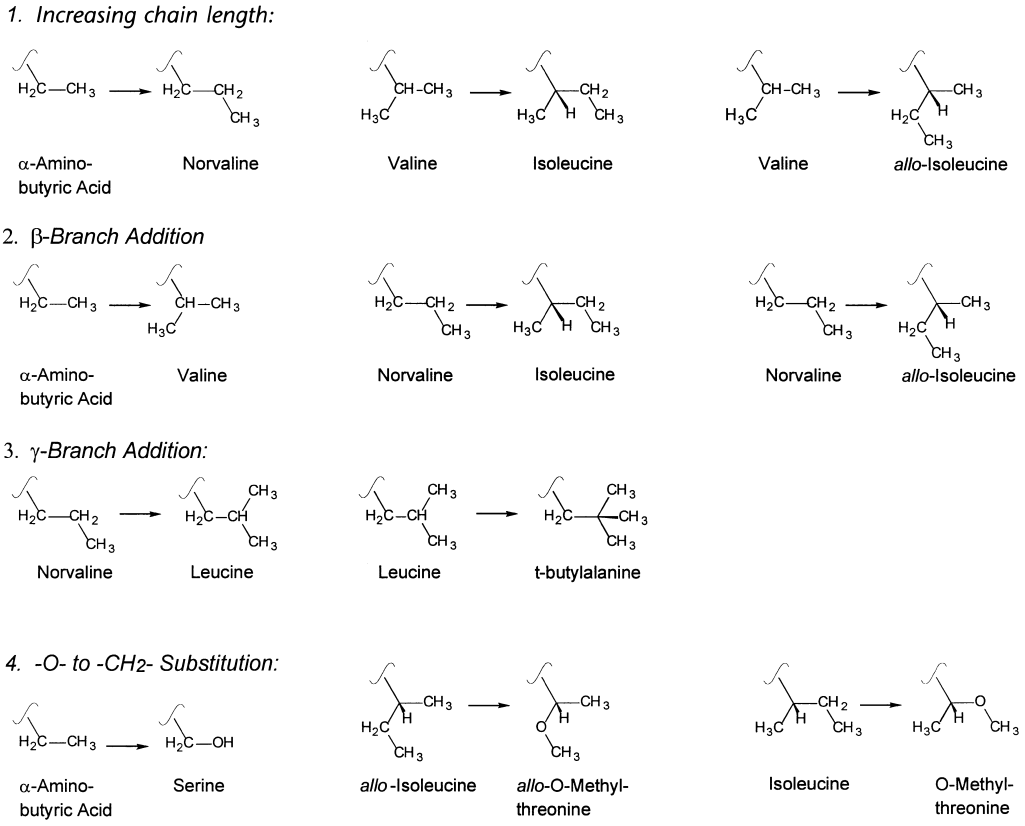

B

	Structural Change	Comparison	β			γ			δ			row averages
1	Increasing chain length	α-Aminobutyric acid to Norvaline	16	27		16	39		20	36		
		Valine to Isoleucine	18	28	*1.8*	35	77	*2.1*	35	15	*1.5*	***1.8***
		Valine to *allo*-Isoleucine	18	39		35	58		35	79		
2	β-branch addition	α-Aminobutyric acid to Valine	16	18		16	35		20	35		
		Norvaline to Isoleucine	27	28	*1.2*	39	77	*1.9*	36	15	*1.5*	***1.5***
		Norvaline to *allo*-Isoleucine	27	39		39	58		36	79		
3	γ-branch addition	Norvaline to Leucine	27	50		39	52		36	49		
		Leucine to *tert*-Butylalanine	50	35	*1.3*	52	59	*1.2*	49	57	*1.3*	***1.3***
		Column average for rows 1 to 3			***1.4***			***1.7***			***1.4***	
4	-O- to -CH2- substitution	Serine to α-Aminobutyric acid	1.5	16		4.5	16		1.2	20		
		O-Methylthreonine to Isoleucine	29	28	*5.0*	23	77	*4.2*	5.3	15	*8.7*	***6.0***
		allo-O-Methylthreonine to *allo*-Isoleucine	12	39		10	58		12	79		

C

	Normal Isomers	β	γ	δ	row average
1	Valine to Isoleucine Norvaline to Isoleucine O-Methylthreonine to Isoleucine	1.2	2.5	1.2	***1.6***
	***allo* isomers**				
2	Valine to *allo*-Isoleucine Norvaline to *allo*-Isoleucine *allo*-O-Methylthreonine to *allo*-Isoleucine	2.3	3.0	3.7	***3.0***

Figure 3. Systematic Effects of Structural Properties on EC_{50}

(A) Structural basis for the 11 comparisons among the residues tested for receptors with single mutations at either the β, γ, or δ subunit.
(B) Tabulation of the trends in EC_{50} for the comparisons in (A). The numbers in plain fonts represent EC_{50} values (μM) for each member of the pair, given in Figure 2. The italicized ratios within dashed boxes are the average for the two or three nearby ratios, corresponding to a given subunit and class of structural change. The ratios in bold italics in the rightmost column are the row averages across subunits for each class of structural change; the ratios in bold italics in the fourth row are column averages for each subunit.
(C) Tabulation of the trends in EC_{50}, grouped by stereochemistry of the stereocenter in the isoleucine side chain.

stereochemistry is analyzed. Figure 3C tabulates EC_{50} ratios for increases in hydrophobicity, classified further by stereochemistry at the stereocenter of the β carbon. The row averages are formed from nine different ratios (though the ratios are not independent) and show clearly that increasing hydrophobicity has a nearly 2-fold

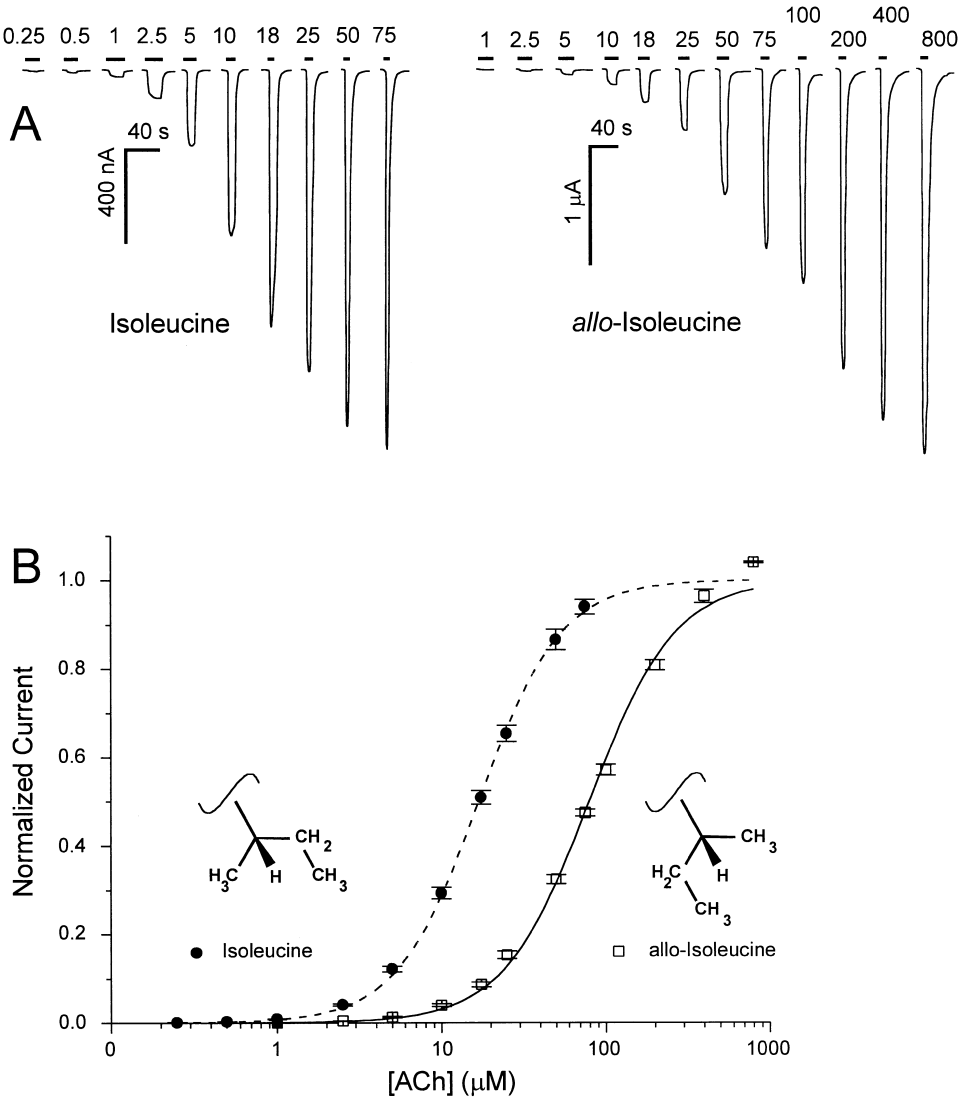

Figure 4. Receptors with Isoleucine or *allo*-Isoleucine at the δ9′ Position Differ by 5-Fold in Their EC_{50} Values

(A) ACh-induced currents for each receptor; ACh concentrations (μM) are given at top.

(B) Dose-response relations. The EC_{50} and n_H values are 15 μM, 1.73 and 79 μM, 1.66 for isoleucine and *allo*-isoleucine, respectively. Data points give mean ± SEM (five cells each).

greater average effect on EC_{50} for the *allo* configuration versus the normal configuration.

The clearest effects of stereochemistry are obtained when one compares isoleucine and *allo*-isoleucine at the δ9′ position; a 5-fold difference in EC_{50} values is seen. Figure 4 presents examples of two-electrode voltage-clamp current measurements, and the complete dose–response relations, for these two receptors. These two side chains differ only in the stereochemical disposition of the β carbon; they have essentially identical values for polarity, hydrophobicity, and volume. Thus, a minimal change in side chain structure produces a marked change in gating properties. The EC_{50} for *allo*-isoleucine exceeds that for isoleucine only in the δ subunit, revealing nonequivalence among subunits at this position in the pore.

The unique role of the δ9′ position is highlighted by comparative data for incorporation of isoleucine or *allo*-isoleucine at the 8′ position, another highly conserved leucine residue. The EC_{50} values for isoleucine and *allo*-isoleucine were 89 and 70 μM at the β subunit, 60 and 63 μM at the γ subunit, and 83 and 71 μM at the δ subunit (data not shown). Thus, the 5-fold difference between normal and *allo* isomer EC_{50} values did not extend to the 8′ position.

We next studied the single-channel properties of the δ9′ *allo*-isoleucine, leucine, and isoleucine receptors (Figure 5) and found that single-channel open times follow the pattern expected from the EC_{50} values; on the other hand, single-channel currents differed by <15% (data not shown). The longer exponential components of average open times, accounting for >85% of the current, were 0.8–1.1 ms for the least sensitive *allo*-isoleucine residue, 1.5–2.0 ms for the wild-type leucine, and 5.5–6.4

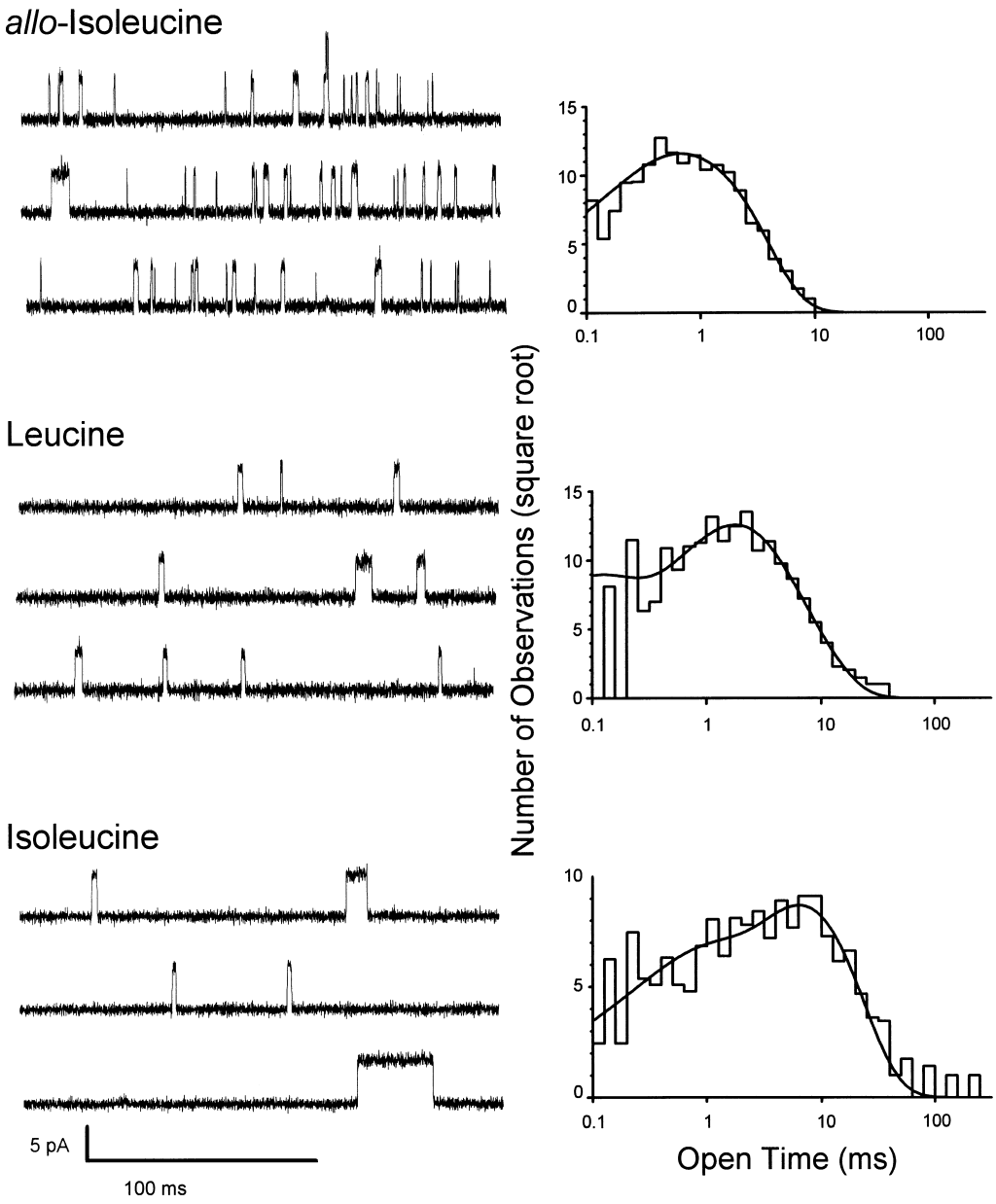

Figure 5. Single-Channel Open Times Correlate with EC_{50} Values

(A) Sample traces from cell-attached patches for oocytes expressing receptors with *allo*-isoleucine, leucine, or isoleucine at the δ9′ position (ACh concentration in the patch pipette was 4, 1, and 1 μM, respectively).

(B) Open-time histograms for representative patches for each receptor. The open times are fit with the exponential components as follows. For the *allo*-isoleucine patch, there were 1504 events; 0.343 ms, 32%; 1.1 ms, 68%. For the WT leucine, there were 1905 events; 0.08 ms, 25%; 1.5 ms, 48%; 3.1 ms, 27%; the weighted average of the longer components is 2.0 ms. For the patch with isoleucine, there were 1148 events; 0.62 ms, 24%; 6.4 ms, 76%. The four openings longer than 90 ms were not observed with each of five other patches from oocytes expressing the isoleucine mutant and have therefore not been fit with an additional component.

ms for the most sensitive isoleucine residue (three patches for each receptor). Thus, the trend in EC_{50} values occurs at least partially because a longer open duration renders the channel more sensitive to ACh.

Stereochemistry Effects Are Modified by 9′ Side Chains in Other Subunits

The effects of stereochemistry on gating at the δ9′ position provide a new tool for studying subunit interactions within the pore. We therefore sought to modify the effects of stereochemistry by mutations at the 9′ position in other subunits.

Previous experiments revealed dramatic effects on gating and channel duration when the 9′ leucine was mutated to serine in any of the subunits (Revah et al., 1991; Filatov and White, 1995; Labarca et al., 1995). EC_{50} decreases by at least 10-fold, and channel duration increases as well. Data presented in Figure 6A show

A EC50 (μM) for Double Mutations at the 9' Position

δ9'residue	No other mutations	α9'Serine	β9'Serine	γ9'Serine
allo-Isoleucine	79	0.63	1.1	8.3
Leucine	49	0.5	1.5	4.5
Isoleucine	15	0.27	0.8	2

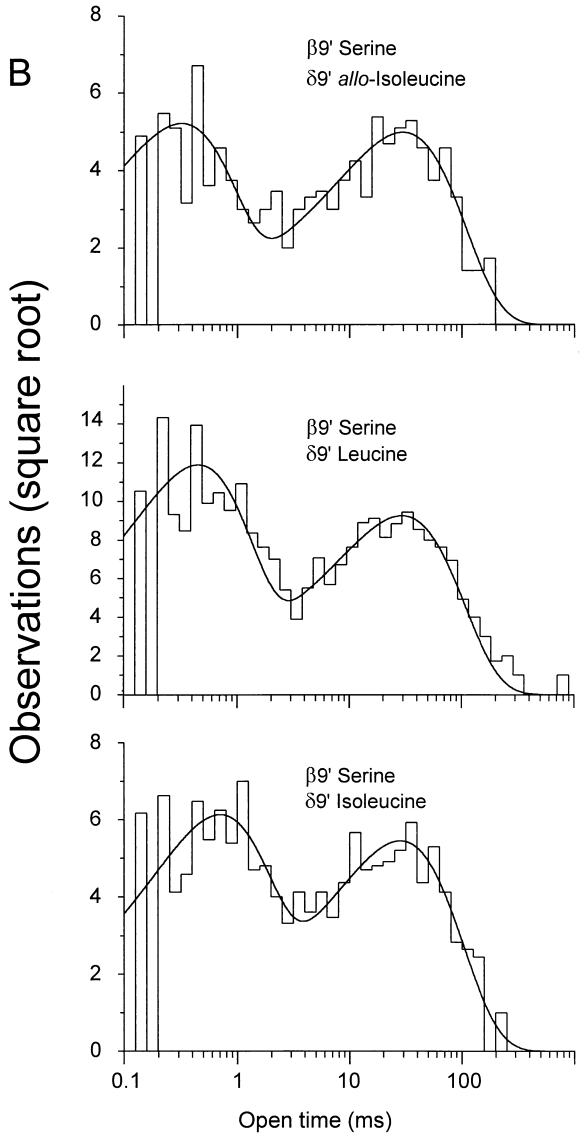

Figure 6. Stereochemistry Effects Are Modified by 9′ Side Chains in Other Subunits

Effects of 9′ leucine to serine mutations at other positions when combined with isoleucine or *allo*-isoleucine at δ9′.

(A) Summary of EC_{50} values for receptors that contain isoleucine, *allo*-isoleucine, or leucine at one 9′ position and serine at another 9′ position.

(B) Open-time histograms for single-channel measurements on β9′serδ9′ile, β9′serδ9′*allo*-ile, and β9′serδ9′leu receptors, measured with 0.4–0.5 μM ACh. Note that the long component of open time is nearly equal for the three receptors, at 28.3, 31.4 and 29.8 ms, respectively. The brief components of open time are 0.67, 0.45, and 0.33 ms, respectively.

that the functional difference between the δ9′ isoleucine and *allo*-isoleucine receptors is modified in characteristic ways by 9′ leucine to serine mutations at other subunits. Thus, when the 9′ leucine to serine mutation is introduced in the β subunit, both the 5-fold EC_{50} difference between δ9′ isoleucine and *allo*-isoleucine and the 5- to 8-fold difference in channel open duration are abolished (Figure 6B). On the other hand, the ~5-fold difference between EC_{50} for isoleucine and *allo*-isoleucine is preserved when the leucine 9′ serine mutation is introduced in the γ subunit. Intermediate changes in EC_{50} are observed when the 9′ leucine to serine mutation is introduced in the two α subunits. These effects do not correlate with the absolute value of the EC_{50}. Among the three receptors studied in Figure 6B, single-channel currents differed by <10% (data not shown).

The large fraction of brief (<1 ms) openings probably represents openings of unliganded or monoliganded channels, which are known to increase for some mutations that introduce hydrophilic residues at the 9′ position (Sigurdson et al., 1994, Biophys. J., abstract; Labarca et al., 1995) and elsewhere in the M2 region (Ohno et al., 1995).

Discussion

Our experiments represent a next stage in the analysis of the structural features that contribute to ion channel gating. In the present study, it is possible to examine the functional consequences of several subtle changes in side chain structure. Overall, the results validate the importance of the hydrophobic nature of the side chain at the 9′ position of the M2 region of the nicotinic receptor. Increasing hydrophobicity, either by adding a CH_2 or by changing an oxygen to a CH_2, increases EC_{50}. Furthermore, the effects of side chain polarity are modified by side chain stereochemistry. In the analysis of Figure 3C, structural changes that decrease polarity have a roughly 2-fold greater average effect on EC_{50} when they result in an *allo* isomer than when they produce a normal isomer.

Although the 9′ leucine residue is generally well conserved in nicotinic ACh and serotonin 5-HT3 receptors, there is at least one example of another residue: the neuronal α5 subunit contains valine at the 9′ position (Boulter et al., 1990; Couturier et al., 1990). In our series of measurements, a single subunit containing a 9′ valine in a heteromultimeric receptor would show an EC_{50} that is, on average, 1.9 times less than the value for a leucine. Our measurements suggest that the valine-containing channel would have a longer open time than the leucine-containing channel.

Special Nature of the δ9′ Substituents

There is a 5-fold difference in EC_{50}, and a parallel change in the open duration, between 9′ isoleucine and 9′ *allo*-isoleucine in the δ subunit of the nAChR. These two side chains are essentially identical in size, shape, and hydrophobicity, differing only in the relative positioning of a methyl versus an ethyl group. Yet the functional difference between these two is equal to the largest changes involving the addition of a new CH_2 group. The

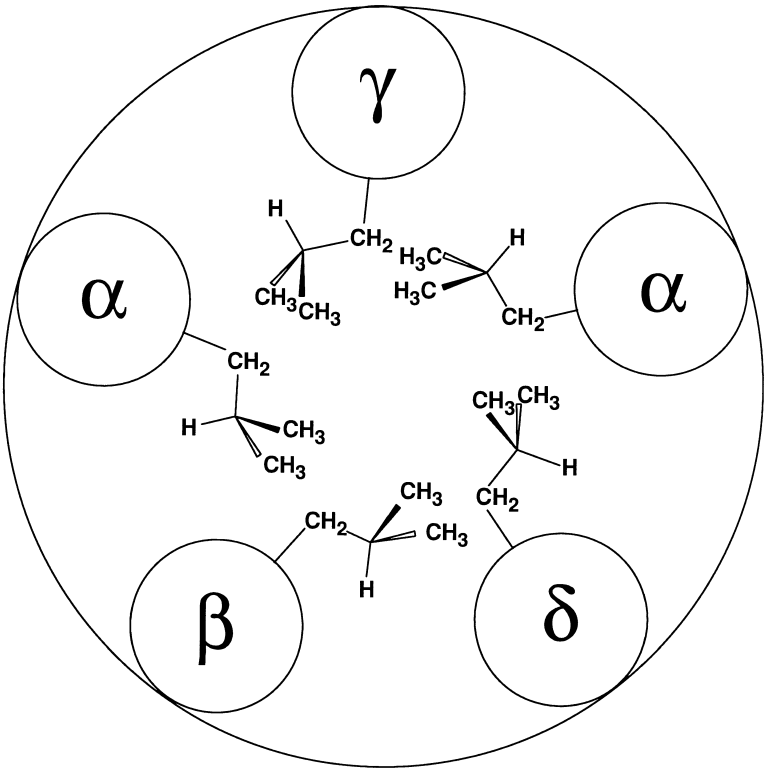

Figure 7. Neighbor Interactions at the Level of the M2 Transmembrane Domains

The present data suggest that the δ subunit is adjacent to the β subunit but not to the γ subunit. Only one of the two α subunits is adjacent to δ, because it is universally accepted that δ is not the unique subunit between the two α subunits. Apparently the α–δ interaction is weaker than the β–δ interaction.

EC_{50} values for incorporation at the δ9′ position differ in the same direction, but less extensively, for O-methylthreonine versus *allo*-O-methylthreonine, which correspond stereochemically to isoleucine and *allo*-isoleucine, respectively. We argue that a subtle structural distinction such as discrimination between normal and *allo* stereoisomers is possible only in a somewhat structured environment.

Our data reveal that the β and, to a lesser extent, α subunit define this special environment. The isoleucine/*allo*-isoleucine difference is essentially abolished by a 9′ leucine to serine mutation in the β subunit; the γ9′ leucine to serine mutation does not significantly alter the δ9′ isoleucine/*allo*-isoleucine effect; the 9′ leucine to serine mutation of both α subunits has an intermediate effect. It seems reasonable to propose that the special pair interaction between β and δ arises from adjacency of the subunits in the receptor structure. That is, the δ subunit is adjacent to the β subunit but not to the γ subunit. The subunit map of Figure 7 describes a disposition that is consistent with our results, leading to the conclusion that the γ subunit lies between the two α subunits. This provides evidence from the pore region that bears on the question of subunit arrangement. The results complement previous data, from ligand binding experiments, that also suggest an α–γ–α arrangement (Karlin et al., 1983; Machold et al., 1995a) and that show important subunit interfaces at the αδ and αγ surfaces (Blount and Merlie, 1989; Sine and Claudio, 1991; Czajkowski et al., 1993). The present data do not agree with the ideas on subunit disposition from the Unwin laboratory (Unwin et al., 1988). In addition, we propose that the β–δ interaction is especially strong relative to other adjacent pairs.

Nature of the β–δ Side Chain Interactions

Increasing side chain polarity at the 9′ position increases the open time of the receptor and decreases EC_{50}. In one proposed model, the 9′ side chains move into a more polar, presumably aqueous, environment in the open state (Akabas et al., 1992; Filatov and White, 1995). We propose specifically that the β9′ and δ9′ side chains contact each other in an aqueous environment in the open state. The greater the overlap between residues, the lower the overall hydrophobic surface area: a stabilizing effect in an aqueous environment. This should result directly in an increased open time and a lower EC_{50}. In the present work, it is hypothesized that the β9′ leucine makes more extensive contacts with a δ9′ isoleucine ($\tau = 6.4$ ms, $EC_{50} = 15$ μM) than with an *allo*-isoleucine ($\tau = 1.1$ ms, $EC_{50} = 79$ μM). Contact with a δ9′ leucine ($\tau = 2.0$ ms, $EC_{50} = 50$ μM) would be of an intermediate extent. The β9′ leucine to serine mutation removes these specific interactions, producing a receptor for which leucine, isoleucine, and *allo*-isoleucine are essentially indistinguishable at δ9′. Our conclusion that the β9′ and δ9′ residues interact strongly with each other in the open state is difficult to reconcile with the proposed gating model in which the 9′ side chains make their closest approach in the closed state (Unwin, 1995).

Molecular Determinants of the Dose–Response Relation

It is at first counterintuitive that EC_{50}, which at least partially reflects agonist-receptor binding, is markedly influenced by mutations in the pore region, thought to lie several nanometers from the binding site (Herz et al., 1989; Unwin, 1993; Machold et al., 1995b). This effect

arises naturally, however, from the fact that these mutations change the channel open time (Figure 5). Two molecules of agonist are thought to remain bound during the entire channel opening, and at least one of these dissociates within 100 μs of channel closing, whichever event (dissociation or closing) occurs first (Nass et al., 1978). Thus, the conformational change that opens the channel also locks agonist onto the binding site; and the mutations affect both the EC_{50} and the binding of agonist, because they affect this conformational change. This point has been confirmed experimentally (Filatov and White, 1995): 9′ leucine to threonine mutations shift EC_{50} for agonists but do not affect the binding of antagonists, presumably because antagonists do not allow the conformational change that opens the channel.

Single-channel measurements establish that the substantial variation in EC_{50} values for the three isomeric side chains leucine, isoleucine, and *allo*-isoleucine at δ9′ are paralleled by changes in open time. In addition, the leveling effect of the β9′ leucine to serine mutation is completely reproduced, in that the three δ9′ structures now have essentially identical channel durations.

Nonetheless, we present here an argument that the changes in open duration are not sufficient to explain fully the shifted dose–response relation. Consider, for example, the 5-fold difference in EC_{50} between isoleucine and *allo*-isoleucine at the δ9′ position. For an [ACh] less than the EC_{50} of either receptor, we measure normalized conductances that differ by a factor of approximately $([ACh]/EC_{50})^{n_H}$, or $5^{1.73} = 16$. Yet, the 5- to 8-fold ratio of channel durations predicts only a 5- to 8-fold ratio of conductances. This suggests that both the open and the closed states are influenced by 9′ mutations, so that increases in open time are also accompanied by modest (2- to 3-fold) decreases in closed time. Conclusions about opening and closing rates are limited by the resolution of the recordings; but recent detailed kinetic studies from our lab, to be presented elsewhere, suggest that channels also open several fold more frequently for several mutations at the 9′ position (H. Zhang, Y. Zhang, C. Labarca, and H. A. Lester, unpublished data).

In summary, the present data highlight both the significant contributions of all five 9′ residues to the control of gating (Filatov and White, 1995; Labarca et al., 1995), emphasizing the major role played by side chain polarity (Filatov and White, 1996, Biophys. J., abstract), and the important departures from symmetry that allow further insights into the details of subunit and side chain interactions. We look forward to still higher resolution chemical and biophysical studies that will shed further light on this fascinating mechanism.

Experimental Procedures

Mutagenesis, mRNA Synthesis, and tRNA Synthesis

Mouse muscle α, β, γ, and δ nAChR subunits containing TAG and/or 9′ leucine to serine mutants were generated using the Clontech Transformer kit and transferred to pAMV, which is optimized for oocyte expression (Nowak et al., 1995). mRNAs for the wild-type and mutant subunits were prepared by in vitro transcription of the appropriate linearized plasmid construct using the Ambion Magic Message machine kit. As before (Nowak et al., 1995), the stop codon in the δ subunit was mutated from TAG to TGA to avoid complications.

The tRNA gene employed was Tetrahymena thermophila $tRNA^{Gln}$ CUA having a G at position 73 (THG73), in the plasmid pTHG73 (Saks et al., 1996). The gene contains an upstream T7 RNA polymerase promoter and a downstream Fok I restriction site. Template DNA for transcription of tRNA lacking the 3′-terminal C75 and A76 was prepared by digesting the plasmid DNA with Fok I restriction endonuclease. In vitro transcription of the linearized DNA template and purification of the truncated THG73 RNA product was performed as previously described (Saks et al., 1996).

Most natural and unnatural amino acids were purchased from Sigma. They were protected and activated as described (Kearney et al., 1996). For the preparation of *allo*-O-methyl threonine, *allo*-threonine was first converted to *allo*-N-NVOC-threonine, followed by treatment with methyliodide to form the corresponding methyl ester. O-methylation was accomplished using methyltriflate (Evans et al., 1994). Hydrolysis of the ester with 1N NaOH was followed by cyanomethylation. The NVOC-protected dCA amino acids were coupled to the THG73 runoff transcript (Sampson and Uhlenbeck, 1988) using T4 RNA ligase. The fraction of ligated product as judged by electrophoresis on high-resolution 8% denaturing polyacrylamide gels was approximately 30% for the THG73 transcripts.

Oocyte Microinjections and Electrophysiological Measurements

Prior to microinjection, the ligated NVOC-aminoacyl-tRNA was renatured by heating to 65°C for 3 min in 1 mM NaOAc (pH 4.5). The NVOC protecting group was subsequently removed by irradiating the sample for 5 min with a 600 W Xenon lamp equipped with WG-335 and UG-11 filters (Schott). For macroscopic dose–response studies, Xenopus oocytes were microinjected (50 nl) with both nAChR mRNA at a concentration ratio of 4:1:1:1 (α:β:γ:δ, 0.42–6.2 ng total mRNA) and the desired acylated tRNA (2.5–10 ng) using published methods (Quick and Lester, 1994). For single channel studies, the 50 nL injection contained nACHR mRNA in a concentration ratio of 2:1:1:4 (10 ng total mRNA) for the δ only mutants and a concentration ratio of 2:4:1:4 (14 ng total mRNA) for β–δ double mutants, as well as 25 to 30 ng of the appropriate acylated tRNA.

Macroscopic measurements were carried out 18–30 hr after injection using a two-electrode voltage-clamp circuit. The extracellular solution contained 5 mM HEPES–NaOH (pH 7.4), 96 mM NaCl, 2 mM KCl, 1 mM $MgCl_2$, and 1 μM atropine to block endogenous muscarinic responses. Macroscopic ACh-induced currents were recorded in response to bath application of the desired agonist concentration at a holding potential of −80 mV. All numerical and plotted data are from measurements obtained for 4–8 individual oocytes. Individual dose–response relations were fit to the Hill equation, $I/I_{max} = I/(1 + \{EC_{50}/[A]\}^{n_H})$ where I is the current for agonist concentration $[A]$, I_{max} is the maximum current, EC_{50} is the concentration to elicit a half-maximum response, and n_H is the Hill coefficient. SEM of EC_{50} measurements was less than 5%.

For single-channel measurements from cell-attached patches, bath and pipette solutions contained 10 mM HEPES–NaOH (pH 7.4), 150 mM KCl, 2 mM $MgCl_2$, and 10 mM EGTA. The concentration of ACh in the pipettes was between 0.4 and 4 μM. The patch was hyperpolarized by 80 mV. Data were recorded with a Geneclamp 500 amplifier (Axon Instruments) and analyzed with pCLAMP 6.0 programs (Axon) using a 5 kHz digital filter.

Acknowledgments

We thank Brad Henkle for help with oocytes and H. Dang, P. England, C. Labarca, M. Nowak, M. E. Saks, J. Sampson, S. Silverman, and Y. Zhang for comments. This work was supported by the National Institutes of Health (NS34407 and NS11756), by the California Tobacco-Related Disease Research Program, and by the Beckman Institute at Caltech.

The costs of publication of this article were defrayed in part by the payment of page charges. This article must therefore be hereby marked *"advertisement"* in accordance with 18 USC Section 1734 solely to indicate this fact.

Received September 13, 1996; revised October 16, 1996.

References

Akabas, M.H., Stauffer, D.A., Xu, M., and Karlin, A. (1992). Acetylcholine receptor channel structure probed in cysteine-substitution mutants. Science *258*, 307–310.

Bertrand, D., Devillers-Thiéry, A., Revah, F., Galzi, J.L., and Hussy, N. (1992). Unconventional pharmacology of a neuronal nicotinic receptor mutated in the channel domain. Proc. Natl. Acad. Sci. USA *89*, 1261–1265.

Blount, P., and Merlie, J.P. (1989). Molecular-basis of the 2 nonequivalent ligand-binding sites of the muscle nicotinic acetylcholine receptor. Neuron *3*, 349–357.

Boulter, J., O'Shea-Greenfield, A., Duvoisin, R.M., Connolly, J.G., Wada, E., Jensen, A., Gardner, P.D., Ballivet, M., Deneris, E.S., McKinnon, D., Heinemann, S., and Patrick, J. (1990). α3, α5, and β4: three members of the rat neuronal nicotinic acetylcholine receptor-related gene family form a gene cluster. J. Biol. Chem. *265*, 4472–4482.

Charnet, P., Labarca, C., Leonard, R.J., Vogelaar, N.J., Czyzyk, L., Gouin, A., Davidson, N., and Lester, H.A. (1990). An open-channel blocker interacts with adjacent turns of α-helices in the nicotinic acetylcholine receptor. Neuron *2*, 87–95.

Couturier, S., Erkman, L., Valera, S., Rungger, D., Bertrand, S., Boulter, J., Ballivet, M., and Bertrand, D. (1990). α5, α3, and non-α3: three clustered avian genes encoding neuronal nicotinic acetylcholine receptor-related subunits. J. Biol. Chem. *265*, 17560–17567.

Czajkowski, C., Kaufmann, C., and Karlin, A. (1993). Negatively charged amino acid residues in the nicotinic receptor delta subunit that contribute to the binding of acetylcholine. Proc. Natl. Acad. Sci. USA *90*, 6285–6289.

Evans, D.A., Ratz, A.M., Huff, B.E., and Sheppard, G.S. (1994). Mild alcohol methylation procedures for the synthesis of polyoxygenated natural-products. Applications to the synthesis of lonomycin-a. Tetrahedron Lett. *35*, 7171–7172.

Filatov, G.N., and White, M.M. (1995). The role of conserved leucines in the M2 domain of the acetylcholine receptor in channel gating. Mol. Pharmacol. *48*, 379–384.

Giraudat, J., Dennis, M., Heidmann, T., Chang, J.-Y., and Changeux, J.-P. (1986). Structure of the high-affinity binding site for noncompetitive blockers of the acetylcholine receptor: serine-262 of the γ subunit is labeled by [^{3}H]chlorpromazine. Proc. Natl. Acad. Sci. USA *83*, 2719–2723.

Herz, J.M., Johnson, D.A., and Taylor, P. (1989). Distance between the agonist and noncompetitive inhibitor sites on the nicotinic acetylcholine receptor. J. Biol. Chem. *264*, 12439–12448.

Karlin, A., and Akabas, M.H. (1995). Toward a structural basis for the function of nicotinic acetylcholine receptors and their cousins. Neuron *15*, 1231–1244.

Karlin, A., Holtzman, E., Yodh, N., Lobel, P., Wall, J., and Hainfeld, J. (1983). The arrangement of the subunits of the acetylcholine receptor of *Torpedo californica*. J. Biol. Chem. *258*, 6678–6681.

Kearney, P., Nowak, N.W., Zhong, W., Silverman, S.K., Lester, H.A., and Dougherty, D.A. (1996). Dose-response relations for unnatural amino acids at the agonist binding site of the nicotinic acetylcholine receptor: tests with novel side chains and with several agonists. Mol. Pharmacol., *50*, 1401–1412.

Labarca, C., Nowak, M.W., Zhang, H., Tang, L., Deshpande, P., and Lester, H.A. (1995). Channel gating governed symmetrically by conserved leucine residues in the M2 domain of nicotinic receptors. Nature *376*, 514–516.

Leonard, R.J., Labarca, C., Charnet, P., Davidson, N., and Lester, H.A. (1988). Evidence that the M2 membrane-spanning region lines the ion channel pore of the nicotinic receptor. Science *242*, 1578–1581.

Machold, J., Utkin, Y., Kirsch, D., Kaufmann, R., Tsetlin, V., and Hucho, F. (1995a). Photolabeling reveals the proximity of the α-neurotoxin binding site to the M2 helix of the ion channel in the nicotinic acetylcholine receptor. Proc. Natl. Acad. Sci. USA *92*, 7282–7286.

Machold, J., Weise, C., Utkin, Y., Tsetlin, V., and Hucho, F. (1995b). The handedness of the subunit arrangement of the nicotinic acetylcholine receptor from Torpedo californica. Eur. J. Biochem. *234*, 427–430.

Nass, M.M., Lester, H.A., and Krouse, M.E. (1978). Response of acetylcholine receptors to photoisomerizations of bound agonist molecules. Biophys. J. *24*, 135–160.

Nowak, M.W., Kearney, P.C., Sampson, J.R., Saks, M.E., Labarca, C.G., Silverman, S.K., Zhong, W., Thorson, J., Abelson, J.N., Davidson, N., Schultz, P.G., Dougherty, D.A., and Lester, H.A. (1995). Nicotinic receptor binding site probed with unnatural amino acid incorporation in intact cells. Science *268*, 439–441.

Ohno, K., Hutchinson, D.O., Milone, M., Brengman, J.M., Bouzat, C., Sine, S.M., and Engel, A.G. (1995). Congenital myasthenic syndrome caused by prolonged acetylcholine receptor channel openings due to a mutation in the M2 domain of the epsilon subunit. Proc. Natl. Acad. Sci. USA *92*, 758–762.

Oiki, S., Koeppe, R.E., II, and Andersen, O.S. (1995). Voltage-dependent gating of an asymmetric gramicidin channel. Proc. Natl. Acad. Sci. USA *92*, 2121–2125.

Quick, M.W., and Lester, H.A. (1994). Methods for expression of excitability proteins in *Xenopus* oocytes. In Ion Channels of Excitable Cells, T. Narahashi, ed. (San Diego: Academic Press), pp. 261–279.

Revah, F., Bertrand, D., Galzi, J.L., Devillers-Thiéry, A., and Mulle, C. (1991). Mutations in the channel domain alter desensitization of a neuronal nicotinic receptor. Nature *353*, 846–849.

Saks, M.E., Sampson, J.R., Nowak, M.W., Kearney, P.C., Du, F., Abelson, N.J., Lester, H.A., and Dougherty, D.A. (1996). An engineered *Tetrahymena* $tRNA^{Gln}$ for *in vivo* incorporation of unnatural amino acids into proteins by nonsense suppression. J. Biol. Chem *271*, 23169–23175.

Sampson, J.R., and Uhlenbeck, O.C. (1988). Biochemical and physical characterization of an unmodified yeast phenylalanine transfer RNA transcribed *in vitro*. Proc. Natl. Acad. Sci. USA *85*, 1033–1037.

Sine, S.M., and Claudio, T. (1991). γ- and δ-subunits regulate the affinity and the cooperativity of ligand binding to the acetylcholine receptor. J. Biol. Chem. *266*, 19369–19377.

Unwin, N. (1995). Acetylcholine receptor channel imaged in the open state. Nature *373*, 37–43.

Unwin, N. (1993). Nicotinic acetylcholine-receptor at 9-angstrom resolution. J. Mol. Biol. *229*, 1101–1124.

Unwin, N., Toyoshima, C., and Kubalek, E. (1988). Arrangement of the acetylcholine receptor subunits in the resting and desensitized states, determined by cryoelectron microscopy of crystallized Torpedo postsynaptic membranes. J. Cell Biol. *107*, 1123–1138.